

Electronic structure and insulating gap in epitaxial VO₂ polymorphs

Shinbuhm Lee, Tricia L. Meyer, Changhee Sohn, Donghwa Lee, John Nichols, Dongkyu Lee, Sung S. Ambrose Seo, John W. Freeland, Tae Won Noh, and Ho Nyung Lee

Citation: *APL Mater.* **3**, 126109 (2015); doi: 10.1063/1.4939004

View online: <http://dx.doi.org/10.1063/1.4939004>

View Table of Contents: <http://scitation.aip.org/content/aip/journal/aplmater/3/12?ver=pdfcov>

Published by the [AIP Publishing](#)

Articles you may be interested in

[Epitaxial growth of VO₂ by periodic annealing](#)

Appl. Phys. Lett. **104**, 063104 (2014); 10.1063/1.4864404

[Comprehensive study of the metal-insulator transition in pulsed laser deposited epitaxial VO₂ thin films](#)

J. Appl. Phys. **113**, 043707 (2013); 10.1063/1.4788804

[Structural, electrical, and terahertz transmission properties of VO₂ thin films grown on c-, r-, and m-plane sapphire substrates](#)

J. Appl. Phys. **111**, 053533 (2012); 10.1063/1.3692391

[In situ x-ray diffraction studies on epitaxial VO₂ films grown on c-Al₂O₃ during thermally induced insulator-metal transition](#)

J. Appl. Phys. **107**, 063503 (2010); 10.1063/1.3327422

[Synthesis and electronic structure of epitaxially stabilized Sr_{2-x}La_xVO₄ \(0x1\) thin films](#)

Appl. Phys. Lett. **82**, 194 (2003); 10.1063/1.1536030

The advertisement features a dark blue background. On the left, the text 'NEW 7400-S Series Vibrating Sample Magnetometers' is displayed in white and yellow. Below this is the Lake Shore Cryotronics logo. In the center, there is an image of the 7400-S Series magnetometer system, which includes a white base unit with two blue sample holders and a computer monitor on top displaying a graph. To the right of the image, the text 'Ideal for the most demanding characterization applications' is written in white, followed by a yellow 'Learn more' button with a play icon.

Electronic structure and insulating gap in epitaxial VO₂ polymorphs

Shinbuhm Lee,¹ Tricia L. Meyer,¹ Changhee Sohn,^{2,3} Donghwa Lee,⁴ John Nichols,¹ Dongkyu Lee,¹ Sung S. Ambrose Seo,⁵ John W. Freeland,⁶ Tae Won Noh,^{2,3} and Ho Nyung Lee^{1,a}

¹*Materials Science and Technology Division, Oak Ridge National Laboratory, Oak Ridge, Tennessee 37831, USA*

²*Center for Correlated Electron Systems, Institute for Basic Science, Seoul 08826, South Korea*

³*Department of Physics and Astronomy, Seoul National University, Seoul 08826, South Korea*

⁴*School of Materials Science and Engineering, Chonnam National University, Gwangju 61186, South Korea*

⁵*Department of Physics and Astronomy, University of Kentucky, Lexington, Kentucky 40506, USA*

⁶*Advanced Photon Source, Argonne National Laboratory, Argonne, Illinois 60439, USA*

(Received 13 October 2015; accepted 14 December 2015; published online 24 December 2015)

Determining the origin of the insulating gap in the monoclinic VO₂(M1) is a long-standing issue. The difficulty of this study arises from the simultaneous occurrence of structural and electronic transitions upon thermal cycling. Here, we compare the electronic structure of the M1 phase with that of single crystalline insulating VO₂(A) and VO₂(B) thin films to better understand the insulating phase of VO₂. As these A and B phases do not undergo a structural transition upon thermal cycling, we comparatively study the origin of the gap opening in the insulating VO₂ phases. By x-ray absorption and optical spectroscopy, we find that the shift of unoccupied *t*_{2g} orbitals away from the Fermi level is a common feature, which plays an important role for the insulating behavior in VO₂ polymorphs. The distinct splitting of the half-filled *t*_{2g} orbital is observed only in the M1 phase, widening the bandgap up to ~0.6 eV. Our approach of comparing all three insulating VO₂ phases provides insight into a better understanding of the electronic structure and the origin of the insulating gap in VO₂. © 2015 Author(s). All article content, except where otherwise noted, is licensed under a Creative Commons Attribution 3.0 Unported License. [<http://dx.doi.org/10.1063/1.4939004>]

Among oxides showing a metal-insulator transition (MIT),^{1–4} VO₂ is one of the most attractive oxides since the MIT occurs near room temperature and is accompanied with large changes in the structural, electronic, and optical properties.^{5–15} Due to the many intriguing phenomena occurring concomitantly with the MIT, unveiling the underlying mechanism of the room temperature MIT in VO₂ has become one of the most studied issues in solid-state physics since its first discovery in a VO₂ single crystal over 50 years ago.^{1,2,16,17} The high temperature metallic phase (R phase) has a rutile structure, in which the nearest-neighbor V–V distance is evenly spaced at 2.88 Å,¹⁶ as shown in Fig. 1(a). The hybridization of V-3*d* and O-2*p* orbitals causes splitting into a doubly degenerate upper state of *e*_g symmetry and a triply degenerate lower state of *t*_{2g} symmetry via the octahedral field.^{16,17} It is naturally expected that the partial occupation of the *t*_{2g} orbitals by the one itinerant electron is the reason for the R phase being metallic, as shown by a schematic energy band diagram in the lower part of Fig. 1(a).

Upon cooling of bulk VO₂ below 340 K, the R phase changes into an insulating monoclinic structure, the so-called M1 phase. In the M1 phase, all V atoms are twisted along the *c*-axis of the rutile

^aElectronic mail: hnyung@ornl.gov

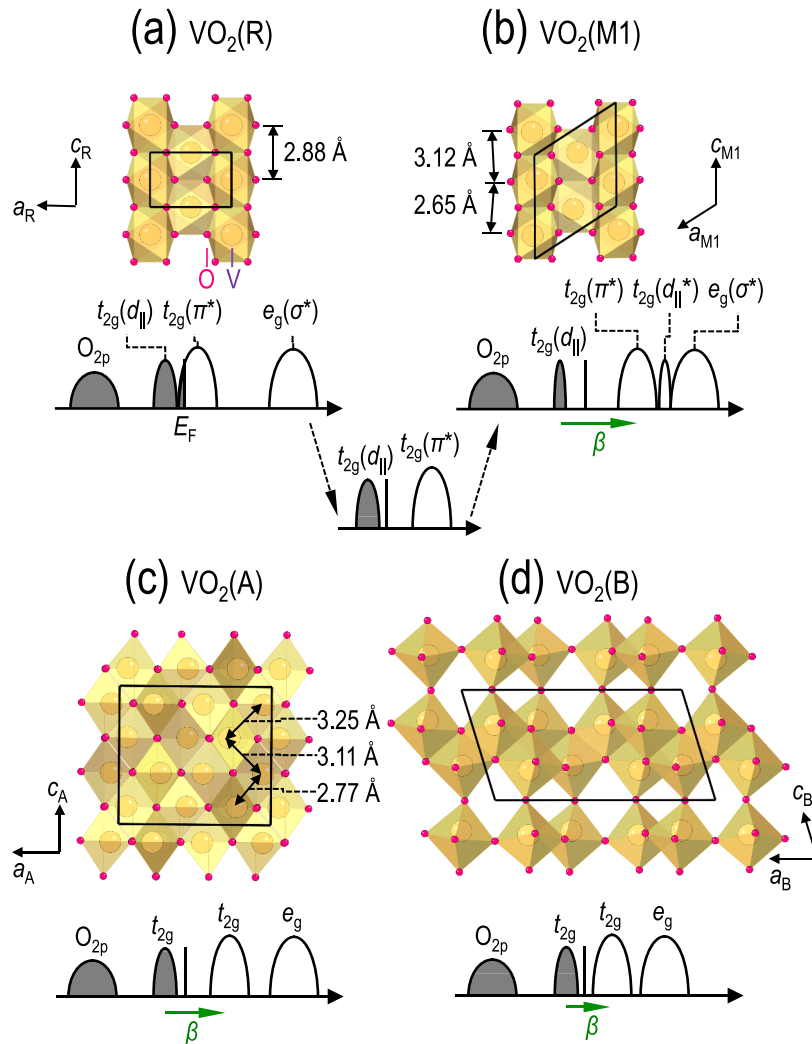


FIG. 1. Schematics of (a) rutile $\text{VO}_2(\text{R})$, (b) monoclinic $\text{VO}_2(\text{M1})$, (c) tetragonal $\text{VO}_2(\text{A})$, and (d) monoclinic $\text{VO}_2(\text{B})$ along with the proposed electronic structures. Solid lines in the schematics indicate the unit cells. Compared with the R phase, in the M1 phase, the half-filled $t_{2g}(d_{||})$ orbital is split into two, and the unoccupied $t_{2g}(\pi^*)$ orbitals are shifted up from the Fermi level. For the change of electronic structures from R to M1 phase, a possible evolution route of the electronic structure is the splitting of the half-filled $t_{2g}(d_{||})$ orbital after the shift of unoccupied $t_{2g}(\pi^*)$ orbitals away from the Fermi level, shown as an intermediate between the two configurations. The electronic structures of insulating A and B phases are proposed at the bottom of (c) and (d). Different from insulating M1 phase, the DOS between t_{2g} and e_g orbitals in the conduction band are not distinctively observed.

framework and paired into uneven chains with V–V separation of 2.65 Å and 3.12 Å distances,¹⁶ as shown in Fig. 1(b). To understand the appearance of the insulating phase in the M1 phase, two competing scenarios have been considered based on the concurrence of structural and electronic transitions. Goodenough proposed one-electron band theory in the framework of a monoclinic distortion.¹⁶ When the V–V distance is less than 2.92–2.94 Å,^{16,18} V–V dimers are formed. As a result, unoccupied t_{2g} orbitals shift up from the Fermi level (E_F), and the localized electron in the V–V dimers split a half-filled t_{2g} orbital into bonding and antibonding bands, introducing an insulating gap, as schematically shown in Fig. 1(b). Goodenough named the unoccupied t_{2g} and e_g orbitals as π^* and σ^* , respectively, since the orbitals form π and σ bonds. In addition, the half-filled t_{2g} orbital was designated as $d_{||}$ band since it is aligned along the one-dimensional V–V chain.¹⁶ However, Zylbersztein and Mott insisted that, even without the monoclinic structure, the half-filled t_{2g} orbital can be split by strong electron correlations if there are small displacements of the V atoms from their atomic positions in the rutile structure.¹⁷ However, the question of “why is the M1 phase insulating?” is not clearly answered,^{7,19–25} owing to

the fact that structural and electronic transitions occur almost simultaneously within a very narrow temperature range (~ 10 K) and within the time scale of picoseconds.^{6,26,27}

To examine each scenario, the key item that must be considered is decoupling of the structural and electronic transitions. For example, the chemical doping of VO₂ with transition metals such as W suppressed the structural transition while the MIT was still observed since the disorder induced by the substitution disturbs the formation of V–V dimers.^{28,29} Additionally, strain has been shown to drive the electronic transition to lower temperature than the structural phase transition in engineered VO₂ nano-/micro-structures³⁰ and VO₂ films grown on (001)-oriented TiO₂ substrates.³¹ These studies indicate that the structural and electronic transitions can be separated from one another but several unanswered questions remain.

Recently, we succeeded in epitaxially synthesizing pure A, B, and M1 phases of VO₂ polymorphs by pulsed laser epitaxy (PLE) and found that the polymorphs are related to each other in the framework of VO₆ octahedra when heated as low as ~ 400 °C.³² The A phase has a tetragonal structure containing VO₆ octahedra, as schematically shown in Fig. 1(c). This phase is highly metastable, so the physical properties and potential for technical applications have not been explored in detail. The B phase has a monoclinic open framework structure, which originates from the edge-sharing VO₆ octahedra,³³ as shown in Fig. 1(d). This open framework made VO₂(B) a good candidate as an energy material, specifically as an electrode in Li-ion batteries.³⁴ Since the resistivity of all phases increases with decreasing temperature,³² it should be noted that all phases have an insulating electronic ground state, thus providing a good playground to investigate the electronic structure without a structural transition. Therefore, here we investigate the electronic structures of insulating A, B, and M1 phases to understand the physical origin of the insulating gap in VO₂. The electronic structures of all VO₂ polymorphs are commonly described by the differences in V–O hybridization. Since both A and B phases do not show a structural phase transition in our measurable temperature range (2–400 K), we can rule out the monoclinic distortion as the origin of the insulating state. In particular, a comparison of A and M1 phases will elucidate the role of V–V dimerization for the insulating gap since zigzag V–V chains in A (3.25, 3.11, and 2.77 Å)³⁵ and M1 (2.65 and 3.12 Å)¹⁶ phases have bonds that are both shorter and longer than Goodenough's insulating critical distance of 2.92–2.94 Å.¹⁸

We grew epitaxial films of phase pure A, B, and M1 phases on (011), (001), and (111)-oriented SrTiO₃ substrates, respectively. In order to obtain high quality thin films with a rocking curve full width at half maximum of less than 0.1°, we optimized the PLE growth parameters, especially for temperature and oxygen partial pressure, and found that the optimal combinations: 420 °C and 10 mTorr for the A phase, 500 °C and 20 mTorr for the B phase, and 450 °C and 15 mTorr for the M1 phase. All films reported here are grown strain-free with thickness of ~ 100 nm in order to minimize substrate-induced strain effects.

To compare the electronic structures in A, B, and M1 phases, we performed X-ray absorption spectroscopy (XAS) at room temperature, which is a powerful tool to study the nature of the unoccupied states in the conduction band.^{11,36–44} Here, we probe the unoccupied states of the t_{2g} and e_g orbitals through the excitation of electrons at the core-level of either the V L -edge ($2p^{3/2}$ or $2p^{1/2}$) or O K -edge ($1s$). Figure 2(a) shows the XAS spectra near the V L -edge. We found three peaks at 515.4, 516.2, and 518.4 eV in the M1 phase, which correspond to the transitions from V $2p_{3/2}$ core-level to $t_{2g}(\pi^*)$, $t_{2g}(d_{||}^*)$, and $e_g(\sigma^*)$, respectively. XAS spectra near the O K -edge are shown in Fig. 2(b). There are also three peaks at 529.6, 530.7, and 531.8 eV, corresponding to the transitions from the O $1s$ core-level to $t_{2g}(\pi^*)$, $t_{2g}(d_{||}^*)$, and $e_g(\sigma^*)$ levels, respectively. These features are consistent with spectra observed for VO₂(M1) single crystals^{36,37,44} and epitaxial films.^{11,45}

On the other hand, in the A and B phases, we observed a broadening of the transitions to t_{2g} and e_g states accompanied by an energy shift of 515.4 (529.6) and 517.9 eV (531.8 eV), respectively. It should be noted that significant peaks were not observed at the energy range near 516.2 eV (530.7 eV), which correspond to the transition to $t_{2g}(d_{||}^*)$ state in the M1 phase. Although the small shift of the V L_3 -peak towards a lower energy for A and B phases may absorb the $t_{2g}(d_{||}^*)$ feature, the data from the O K edge indicates that any splitting of the half-filled t_{2g} orbital might be weak and may not play a significant role for the insulating behavior in the A and B phases. This distinct difference might occur since the A phase contains longer (more weakly bonded) V–V chains (2.77 Å) than the M1 phase (2.65 Å).

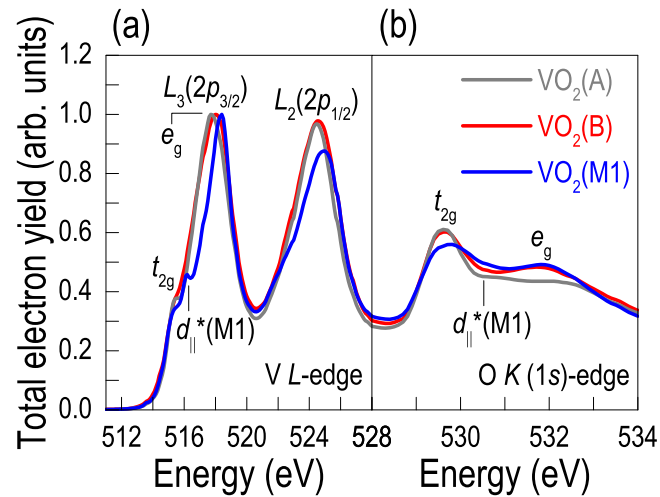


FIG. 2. X-ray absorption spectroscopy of (a) V *L*-edge and (b) O *K*-edge in insulating A, B, and M1 phases collected at room temperature. The transitions from the core-levels to the V *L*-edge and O *K*-edge occur at 512–528 eV and 528–534 eV, respectively. Indices of t_{2g} , $d_{||}^*$ (M1), and e_g indicate the transition from the core-levels to unoccupied t_{2g} , $d_{||}^*$ (M1), and e_g orbitals in the conduction band, respectively. The transition to $d_{||}^*$ -band is observed only in the M1 phase.

The other model discussed above regarding the origin of the insulating gap in the A, B, and M1 phases is the shift of unoccupied t_{2g} bands away from the Fermi level. As shown by a schematic energy diagram in Fig. 1(b), the insulating gap in the M1 phase corresponds to the energy gap between the valence band maximum ($t_{2g}(d_{||})$ band) and the conduction band minimum ($t_{2g}(\pi^*)$ band). In order to elucidate such a bandgap opening, we measured the optical conductivity σ_1 by optical reflectivity and ellipsometry in the photon energy range of 0.1–3 eV, as shown in Fig. 3. The optical bandgap was determined by the extrapolation to zero of the linear portion of the sharp rise

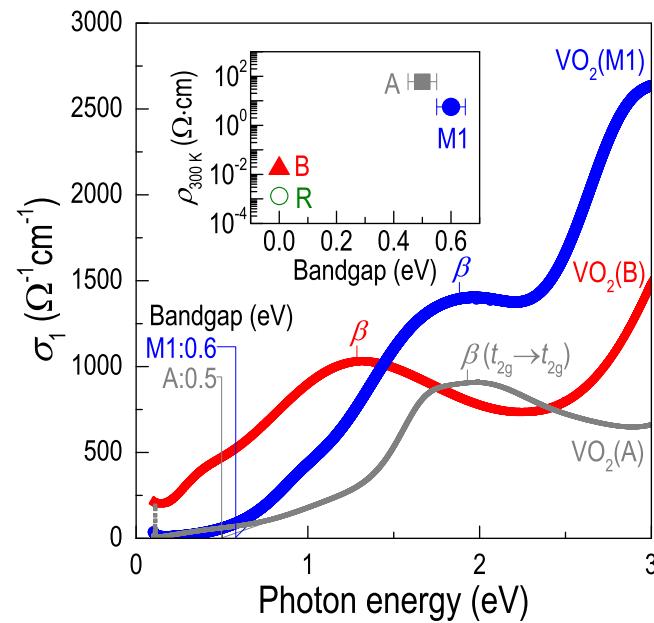


FIG. 3. Optical spectra and bandgaps of M1, A, and B phases. By measuring optical conductivity σ_1 , we obtained the bandgap energy to be 0.6 ± 0.05 eV for M1 and 0.5 ± 0.05 eV for A. The β -peaks, corresponding to the optical transition from the valence band maximum to the conduction band minimum, as denoted in Fig. 1, are downshifted from M1 and A to B, indicating a downshift of unoccupied t_{2g} orbitals with respect to the Fermi level. The resistivity of VO_2 polymorphs largely increases with a small increase in the bandgap, as shown in the inset. For comparison, we include the room temperature resistivity value of metallic R phase.

of σ_1 curve. We further note that the non-zero σ_1 below the bandgap in A and M1 phases can be attributed to thermal broadening, incoherent spectral weight in the gap, or a data fitting artifact.^{46–48} We obtained the optical bandgap of 0.6 ± 0.05 eV for the M1 phase, as indicated by a solid line, which is comparable to the bulk value of ~ 0.6 eV.⁷ The bandgap of the A phase was 0.5 ± 0.05 eV. As we will show later, the optical bandgaps obtained here are consistent with hybrid functional calculations, validating our gap assignment. This optical result indicates that the optical bandgap of the A phase is similar to (if not, slightly smaller than) that of the M1 phase although splitting of the half-filled t_{2g} orbital was not clearly observed for the A phase. More interestingly, the optical conductivity of the B phase maintains non-zero spectral weight at low photon energy, which means that there is a meaningful density of states inside the bandgap. Therefore, the B phase might be a narrow bandgap (<25 meV at room temperature) material, in which the electrons in the valence band can thermally jump into the conduction band at room temperature.

We have found that the resistivity in insulating VO₂ is more sensitive to the separation of the unoccupied t_{2g} orbitals from the Fermi level than the splitting of the half-filled t_{2g} orbital. The inset in Fig. 3 shows the relationship between the optical bandgap of VO₂ polymorphs and their resistivity measured at 300 K by the four-point probe method. The resistivity increases as the bandgap becomes larger. The β -peaks, which correspond to the transition from the valence band maximum to the conduction band minimum, shifted monotonically to higher photon energies in the order of B to M1 and A phases. This trend indicates that the unoccupied t_{2g} orbitals move further from the Fermi level when the phase of VO₂ becomes more insulating. Conversely, if there were appreciable effects from splitting of the half-filled t_{2g} orbital, one would expect a narrower bandwidth in the half-filled t_{2g} orbital and thus a larger gap energy and resistivity, which are consistent with our optical data presented here. Thus, both XAS and optical measurements support that the insulating nature of VO₂ arises basically from the shift of unoccupied t_{2g} orbitals away from the Fermi energy.

As discussed above, one of the major questions for understanding the insulating nature of the M1 phase is identifying which mechanism, i.e., whether the one-electron or correlated-electron description, is responsible for this ground state.^{1,2,16,17} To address this issue, we calculated the density of states (DOSs) for the A, B, and M1 phases of VO₂ using density functional theory (DFT)⁴⁹ and accurate hybrid functional calculations.⁵⁰ While the former is based on the one-electron aspect,¹⁹ the latter includes the correlated-electron effects and, thus, can improve the underestimated DFT bandgap originating from the well-known self-interaction error. The hybrid functional calculation was performed within the PBE0 functional,⁵⁰ which mixes 15% of Hartree-Fock exchange into DFT as implemented in the Vienna *ab initio* simulation package (VASP) code.⁵¹ Periodic boundary condition and Monkhorst-Pack k-point sampling⁵² with a grid of up to $8 \times 8 \times 8$ was used for the Brillouin zone integration.

Based on the hybrid functional calculations shown in Fig. 4, we have found that the calculations of DOS describe well the insulating gap in A and M1 phases when the correlated-electron effects are taken into account. For example, our DFT calculations without considering the correlated-electron contribution predicted signatures of a metallic ground state for the A, B, and M1 phases, in agreement with previous studies for the M1 phase that determined a bandgap of 0.04 eV,¹⁹ much smaller than the experimental value of 0.6 eV.⁷ These previous discrepancies imply that DFT calculations without considering the correlated-electron contribution do not accurately describe the electronic ground states of VO₂ systems. On the other hand, when we consider the correlated-electron effects using the hybrid calculation, which is known to be more accurate than normal DFT,⁵⁰ we find that A and M1 are insulating, while the B phase is a narrow bandgap semiconductor, similar to our optical spectroscopy results. Figure 4 shows the total DOS of the M1, A, and B phases, which were calculated by hybrid functional method. For the conduction band, the DOS between t_{2g} and e_g is only observed for the M1 phase near 1.5 eV and is consistent with our XAS measurements. Moreover, our theoretical calculations indicate that the bandgaps of the A and M1 phases are 0.5 and 0.6 eV, respectively, while that of the B phase is almost negligible. Therefore, the good agreement between our hybrid functional calculations and experimental observations strongly suggests that correlated-electron effects are driving the insulating properties observed in these VO₂ systems. We represent the overall electronic structure of A and B phases in the lower parts of Figs. 1(c) and 1(d), respectively.

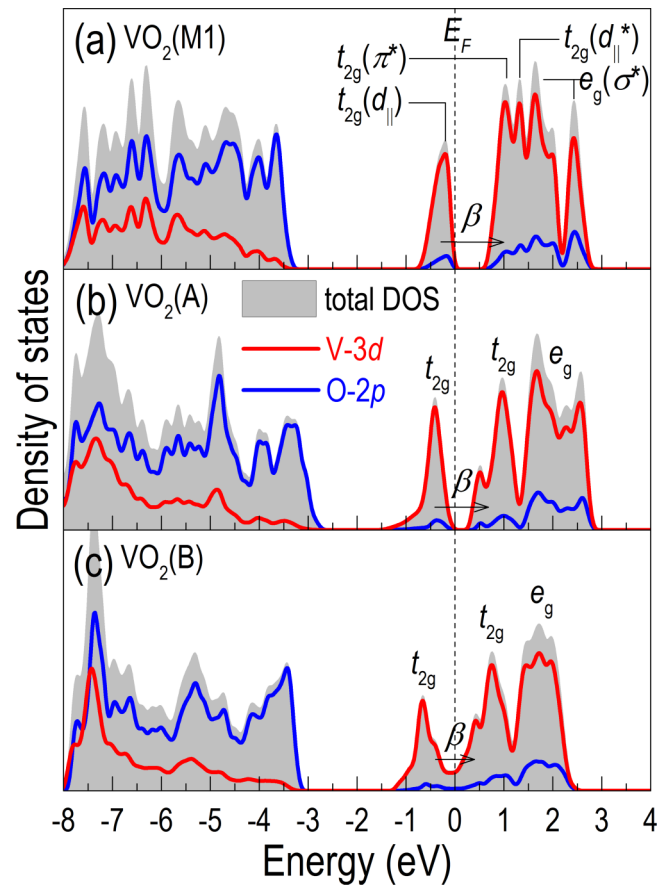


FIG. 4. Density of states determined from hybrid functional calculations of (a) M1, (b) A, and (c) B phases. For clarity, we focused on the DOS near the Fermi level (0 eV), which include t_{2g} and e_g orbitals. The $d_{||}^*$ -band is clearly seen near 1.5 eV between the unoccupied $t_{2g}(\pi^*)$ and $e_g(\sigma^*)$ orbitals in M1 phase. While the M1 and A phases have bandgaps of 0.6 and 0.5 eV, respectively, the bandgap of B is smaller than the thermal excitation energy at room temperature (25 meV).

In conclusion, by comparing the electronic structure of electronically insulating A, B, and M1 phases, we found that the shift of unoccupied t_{2g} orbitals away from the Fermi level was critical for the formation of insulating gaps in each VO_2 phase. A splitting of the half-filled t_{2g} orbital decreases its bandwidth; therefore, the bandgap of the M1 phase increases further, yielding a more insulating state. Our theoretical calculations indicated that the appearance of insulating properties could be attributed to the correlated-electron effects. Therefore, our systematic comparison of the electronic structure of the M1 phase with that of other insulating VO_2 phases, including A and B phases, provides clear insights into understanding the long-standing issue on the insulating gap in VO_2 .

This work was supported by the U.S. Department of Energy, Office of Science, Basic Energy Sciences, Materials Sciences and Engineering Division. Work for optical spectroscopy was supported by No. IBS-R009-D1. Computational work was supported by the National Institute of Supercomputing and Network/Korea Institute of Science and Technology Information with supercomputing resources including technical support No. KSC-2015-C3-034. Spectroscopic ellipsometry at the University of Kentucky was supported by the National Science Foundation grant DMR-1454200. Work at the Advanced Photon Source was supported by the U.S. Department of Energy, Office of Science, Office of Basic Energy Sciences, under Contract No. DE-AC02-06CH11357.

¹ Z. Yang, C. Y. Ko, and S. Ramanathan, in *Annual Review of Materials Research*, edited by D. R. Clarke and P. Fratzl (Annual Reviews, Palo Alto, 2011), Vol. 41, pp. 337–367.

² M. Imada, A. Fujimori, and Y. Tokura, *Rev. Mod. Phys.* **70**(4), 1039–1263 (1998).

³ E. Dagotto, *Science* **309**(5732), 257–262 (2005).

⁴ D. N. Basov, R. D. Averitt, D. van der Marel, M. Dressel, and K. Haule, *Rev. Mod. Phys.* **83**(2), 471–541 (2011).

- ⁵ J. Jeong, N. Aetukuri, T. Graf, T. D. Schladt, M. G. Samant, and S. S. P. Parkin, *Science* **339**(6126), 1402–1405 (2013).
- ⁶ V. R. Morrison, R. P. Chatelain, K. L. Tiwari, A. Hendaoui, A. Bruhacs, M. Chaker, and B. J. Siwick, *Science* **346**(6208), 445–448 (2014).
- ⁷ M. M. Qazilbash, M. Brehm, B. G. Chae, P. C. Ho, G. O. Andreev, B. J. Kim, S. J. Yun, A. V. Balatsky, M. B. Maple, F. Keilmann, H. T. Kim, and D. N. Basov, *Science* **318**(5857), 1750–1753 (2007).
- ⁸ P. Baum, D. S. Yang, and A. H. Zewail, *Science* **318**(5851), 788–792 (2007).
- ⁹ T. Driscoll, H. T. Kim, B. G. Chae, B. J. Kim, Y. W. Lee, N. M. Jokerst, S. Palit, D. R. Smith, M. Di Ventra, and D. N. Basov, *Science* **325**(5947), 1518–1521 (2009).
- ¹⁰ M. Nakano, K. Shibuya, D. Okuyama, T. Hatano, S. Ono, M. Kawasaki, Y. Iwasa, and Y. Tokura, *Nature* **487**(7408), 459–462 (2012).
- ¹¹ N. B. Aetukuri, A. X. Gray, M. Drouard, M. Cossale, L. Gao, A. H. Reid, R. Kukreja, H. Ohldag, C. A. Jenkins, E. Arenholz, K. P. Roche, H. A. Durr, M. G. Samant, and S. S. P. Parkin, *Nat. Phys.* **9**(10), 661–666 (2013).
- ¹² J. D. Budai, J. W. Hong, M. E. Manley, E. D. Specht, C. W. Li, J. Z. Tischler, D. L. Abernathy, A. H. Said, B. M. Leu, L. A. Boatner, R. J. McQueeney, and O. Delaire, *Nature* **515**(7528), 535–539 (2014).
- ¹³ M. K. Liu, H. Y. Hwang, H. Tao, A. C. Strikwerda, K. B. Fan, G. R. Keiser, A. J. Sternbach, K. G. West, S. Kittiwatanakul, J. W. Lu, S. A. Wolf, F. G. Omenetto, X. Zhang, K. A. Nelson, and R. D. Averitt, *Nature* **487**(7407), 345–348 (2012).
- ¹⁴ J. H. Park, J. M. Coy, T. S. Kasirga, C. M. Huang, Z. Y. Fei, S. Hunter, and D. H. Cobden, *Nature* **500**(7463), 431–434 (2013).
- ¹⁵ S. Lee, T. L. Meyer, S. Park, T. Egami, and H. N. Lee, *Appl. Phys. Lett.* **105**(22), 4 (2014).
- ¹⁶ J. B. Goodenough, *J. Solid State Chem.* **3**(4), 490–500 (1971).
- ¹⁷ A. Zylbersztejn and N. F. Mott, *Phys. Rev. B* **11**(11), 4383–4395 (1975).
- ¹⁸ J. B. Goodenough, *Czech J. Phys.* **17**(4), 304–336 (1967).
- ¹⁹ R. M. Wentzcovitch, W. W. Schulz, and P. B. Allen, *Phys. Rev. Lett.* **72**(21), 3389–3392 (1994).
- ²⁰ T. M. Rice, H. Launois, and J. P. Pouget, *Phys. Rev. Lett.* **73**(22), 3042 (1994).
- ²¹ S. A. Corr, D. P. Shoemaker, B. C. Melot, and R. Seshadri, *Phys. Rev. Lett.* **105**(5), 4 (2010).
- ²² E. Arcangeletti, L. Baldassarre, D. Di Castro, S. Lupi, L. Malavasi, C. Marini, A. Perucchi, and P. Postorino, *Phys. Rev. Lett.* **98**(19), 4 (2007).
- ²³ H. T. Kim, Y. W. Lee, B. J. Kim, B. G. Chae, S. J. Yun, K. Y. Kang, K. J. Han, K. J. Yee, and Y. S. Lim, *Phys. Rev. Lett.* **97**(26), 4 (2006).
- ²⁴ C. Weber, D. D. O'Regan, N. D. M. Hine, M. C. Payne, G. Kotliar, and P. B. Littlewood, *Phys. Rev. Lett.* **108**(25), 5 (2012).
- ²⁵ A. S. Belozarov, M. A. Korotin, V. I. Anisimov, and A. I. Poteryaev, *Phys. Rev. B* **85**(4), 10 (2012).
- ²⁶ D. Wegkamp, M. Herzog, L. Xian, M. Gatti, P. Cudazzo, C. L. McGahan, R. E. Marvel, R. F. Haglund, A. Rubio, M. Wolf, and J. Stahler, *Phys. Rev. Lett.* **113**(21), 5 (2014).
- ²⁷ A. Cavalleri, T. Dekorsy, H. H. W. Chong, J. C. Kieffer, and R. W. Schoenlein, *Phys. Rev. B* **70**(16), 4 (2004).
- ²⁸ K. Shibuya, M. Kawasaki, and Y. Tokura, *Appl. Phys. Lett.* **96**(2), 3 (2010).
- ²⁹ E. Sakai, K. Yoshimatsu, K. Shibuya, H. Kumigashira, E. Ikenaga, M. Kawasaki, Y. Tokura, and M. Oshima, *Phys. Rev. B* **84**(19), 5 (2011).
- ³⁰ Z. S. Tao, T. R. T. Han, S. D. Mahanti, P. M. Duxbury, F. Yuan, C. Y. Ruan, K. Wang, and J. Q. Wu, *Phys. Rev. Lett.* **109**(16), 5 (2012).
- ³¹ J. Laverock, S. Kittiwatanakul, A. A. Zakharov, Y. R. Niu, B. Chen, S. A. Wolf, J. W. Lu, and K. E. Smith, *Phys. Rev. Lett.* **113**(21), 5 (2014).
- ³² S. Lee, I. N. Ivanov, J. K. Keum, and H. N. Lee, e-print [arXiv:1509.00525](https://arxiv.org/abs/1509.00525) [cond-mat.mtrl-sci] (2015).
- ³³ C. Leroux, G. Nihoul, and G. Van Tendeloo, *Phys. Rev. B* **57**(9), 5111–5121 (1998).
- ³⁴ W. Li, J. R. Dahn, and D. S. Wainwright, *Science* **264**(5162), 1115–1118 (1994).
- ³⁵ S. R. Popuri, A. Artemenko, C. Labrugere, M. Miclau, A. Villesuzanne, and M. Pollet, *J. Solid State Chem.* **213**, 79–86 (2014).
- ³⁶ M. W. Haverkort, Z. Hu, A. Tanaka, W. Reichelt, S. V. Streltsov, M. A. Korotin, V. I. Anisimov, H. H. Hsieh, H. J. Lin, C. T. Chen, D. I. Khomskii, and L. H. Tjeng, *Phys. Rev. Lett.* **95**(19), 4 (2005).
- ³⁷ T. C. Koethe, Z. Hu, M. W. Haverkort, C. Schussler-Langeheine, F. Venturini, N. B. Brookes, O. Tjernberg, W. Reichelt, H. H. Hsieh, H. J. Lin, C. T. Chen, and L. H. Tjeng, *Phys. Rev. Lett.* **97**(11), 4 (2006).
- ³⁸ N. F. Quackenbush, J. W. Tashman, J. A. Mundy, S. Sallis, H. Paik, R. Misra, J. A. Moyer, J. H. Guo, D. A. Fischer, J. C. Woicik, D. A. Muller, D. G. Schlom, and L. F. J. Piper, *Nano Lett.* **13**(10), 4857–4861 (2013).
- ³⁹ L. Whittaker, C. Jaye, Z. G. Fu, D. A. Fischer, and S. Banerjee, *J. Am. Chem. Soc.* **131**(25), 8884–8894 (2009).
- ⁴⁰ D. Ruzmetov, S. D. Senanayake, V. Narayanamurti, and S. Ramanathan, *Phys. Rev. B* **77**(19), 5 (2008).
- ⁴¹ D. Ruzmetov, S. D. Senanayake, and S. Ramanathan, *Phys. Rev. B* **75**(19), 7 (2007).
- ⁴² A. Cavalleri, M. Rini, H. H. W. Chong, S. Fourmaux, T. E. Glover, P. A. Heimann, J. C. Kieffer, and R. W. Schoenlein, *Phys. Rev. Lett.* **95**(6), 4 (2005).
- ⁴³ X. G. Tan, T. Yao, R. Long, Z. H. Sun, Y. J. Feng, H. Cheng, X. Yuan, W. Q. Zhang, Q. H. Liu, C. Z. Wu, Y. Xie, and S. Q. Wei, *Sci. Rep.* **2**, 6 (2012).
- ⁴⁴ M. Abbate, F. M. F. Degroot, J. C. Fuggle, Y. J. Ma, C. T. Chen, F. Sette, A. Fujimori, Y. Ueda, and K. Kosuge, *Phys. Rev. B* **43**(9), 7263–7267 (1991).
- ⁴⁵ J. Laverock, L. F. J. Piper, A. R. H. Preston, B. Chen, J. McNulty, K. E. Smith, S. Kittiwatanakul, J. W. Lu, S. A. Wolf, P. A. Glans, and J. H. Guo, *Phys. Rev. B* **85**(8), 5 (2012).
- ⁴⁶ W. S. Choi, M. F. Chisholm, D. J. Singh, T. Choi, G. E. Jellison, and H. N. Lee, *Nat. Commun.* **3**, 6 (2012).
- ⁴⁷ T. Arima, Y. Tokura, and J. B. Torrance, *Phys. Rev. B* **48**(23), 17006–17009 (1993).
- ⁴⁸ H. B. Zhang, K. Haule, and D. Vanderbilt, *Phys. Rev. Lett.* **111**(24), 5 (2013).
- ⁴⁹ W. Kohn and L. J. Sham, *Phys. Rev.* **140**(4A), 1133–1138 (1965).
- ⁵⁰ A. D. Becke, *J. Chem. Phys.* **96**(3), 2155–2160 (1992).
- ⁵¹ G. Kresse and J. Furthmüller, *Comput. Mater. Sci.* **6**(1), 15–50 (1996).
- ⁵² H. J. Monkhorst and J. D. Pack, *Phys. Rev. B* **13**(12), 5188–5192 (1976).